# Geochemical and Mineralogical Investigation of Kaolin Occurrence around Ugiamen Area, Southern Nigeria

Oyebamiji Abiola1,2,3, Hu Ruizhong1,Falae Philips4 and Okunlola Olugbenga5
1StateKey Laboratory of Ore Deposit Geochemistry, Institute of Geochemistry, Chinese Academy of Sciences, Guiyang 550081, China
2University of Chinese Academy of Sciences, Beijing 100049, China
3Ekiti State University, Ado-Ekiti, Nigeria
4Central Building Research Institute CBRI, Roorkee, India
5University of Ibadan, Ibadan, Nigeria
Email address: abeylove2003@yahoo.com

**Abstract :** Geological, mineralogical and geochemical studies were carried out on twelve kaolin samples around Ugiamen area, southern Nigeria in order to determine their characteristics, the ore genesis and possibly economic viability of the deposit. Quantitative and qualitative mineralogical investigations reveal kaolinite as the predominant mineral followed by quartz and muscovite as accessory minerals. There is gradual transition zone between the kaolin and its parent rocks which shows the residual origin of the kaolin. Variable amount of major oxides such as Mgo, CaO and Na2O were lost as a result of the weathering process, whereas SiO2, Al2O3, LOI and LREE were enriched in the residual kaolin. Chondrite-normalized REE pattern of the kaolin samples shows an overall enrichment of LREE and depletion of HREE, also slightly negative Eu-anomaly probably originated from the parent rocks. The findings of the present study indicate evident characteristic feature of intense weathering and also the influence of the acidic nature of the source rock in the study area.

**Key word:** Kaolin · Mineralogical · Geochemical · Ugiamen · Weathering



## 1. Introduction

Kaolin is one of the major valuable, versatile and widely used industrial minerals. Kaolin is a hydrated aluminium silicate ($Al_2SiO_5(OH)_4$) which is used industrially for the production of many materials with significant economic importance(Rashad, 2013). They are found in commercial quantity in most sedimentary basins as a product of weathering or hydrothermal alteration of rocks containing aluminosilicate minerals. They are primarily composed of aluminium, silicon, oxygen, ferrous and ferric iron and hydroxyl groups. Other elements such as potassium, calcium, phosphorus, sodium, magnesium also occur in various proportions.

In the last decade, the kaolin industry has experienced difficult times due to over-production in Europe and the USA. The emergence of major new high quality kaolin sources in Brazil and Australia, and the constantly increasing supply of low-grade materials, has also affected the market. However, with increasingand new industrial applications of kaolin, any strategically located promising deposit is worth exploiting, especially so in the developing world.

The most important members of the kaolin family include dickite, nacrite, allophone and hallosite. Physically, they occur usually as white to near white in colour; they are earthy to dull with plastic touch. The characteristics and chemical composition of a kaolin deposit usually determines its industrial utilisation. Industrial uses of kaolin include; paper filling and coating; plastic, paint, rubber manufacturing (as reinforcing agent); adhesive and ink pigment, ceramic raw materials for porcelain, dinnerware; tiles and enamels; catalyst for petroleum and auto exhaust emission catalytic control devices; digestive coating remedy and cosmetics base.

Other unique industrial applications include; acts as a suitable medium for moulding mixture in cast iron and steel foundry, and insulator refractories where the most important properties are plasticity, strength and fired colour. In Nigeria, kaolin deposits are found in the Anambra, Chad, Bida, Benue Trough and the Niger Delta Basin (Akhirevbulu and Ogunbajo, 2011). Despite their abundance in Nigeria, the major problems associated with the quarrying of kaolin in these areas include caving in of holes, influx of groundwater particularly in the rainy season and the presence of impurities such as quartz, feldspar, tourmaline, muscovite etc. Thus, the objective of this paper is to carry out a detailed geological, geochemical and mineralogical characterization of kaolinite deposits occurring in part of Ugiamen in Edo State in evaluating their viability of the deposit. Possible applications in industry are suggested.



## 2. Materials and Methods

For this study, twelve kaolin samples were collected from well exposed clay lithologic units of the formations, while pitting was adopted in grid pattern where there was poor exposure of clay. Sampling was done at different vertical intervals along some selected holes drilled in the course of exploration.

Geochemical and mineralogical analysis were performed at the Bureau Veritas Commodities (Vancouver, Canada) by emission spectrometry using Inductively Coupled Plasma and Atomic Emission source (ICP-AES) for major elements and mass spectrometry (ICP-MS) for trace elements and rare earths, after fusion with $LiBO_2$ and dissolution in $HNO_3$.

X-ray Diffraction (XRD) analysis was used to determine mineralogical composition of the kaolin sample as described by Bundy (1993), and Murray and Keller (1993).

## 3. Description and Geology of the area of study

The area lies between longitude $6^0$01’00’’E- $6^0$05’00’’E and latitude $6^0$39’00’’N- $6^0$43’00’’N with total surface area of about 51.2km$^2$. The area is traversed by a major road that trends SE through Okemuen to Ugiamen and also northwards through Ekpoma to Ugiamen (Fig. 1). The area is underlained by claystone (kaolin) with interbedded with layers of lignite at varying thickness. (Fig.2 and 3).

The formation of the southern Nigerian sedimentary basin began during the Early Cretaceous (Albian) following the basement subsidence along the Benue and Niger Troughs (Nwachukwu, 1972; Olade, 1975). Folding and uplift occurred in the Santonian along a northeast-southwest trending axis in the Abakaliki-Benue area. The Anambra platform, lying to the west and southwest of the Abakaliki folded belts, subsided to form the Anambra basin (Reyment, 1965; Short and Stauble, 1967; Murat, 1972; Benkhelil, 1989) (Fig. 4).

The paralicOgwashi-Asaba Formation (Oligocene-Miocene) is an important lithostratigraphic unit of the Anambra basin; it is underlained by the regression Ameki formation (Early Eocene) and overlain by Miocene-Recent Benin formation. The Ogwashi-Asaba formation consists of a sequence of coarse-grained sandstone, light coloured clays and carbonaceous shale within which are intercalations of lignite seams of continental origin (Kogbe, 1976; Jan du Chene et al., 1978, Ogala, 2011). Reyment (1965) suggested an Oligocene-Miocene age for the Ogwashi- Asaba formation, but palynological study by Jan du Chene et al. (1978) yielded a Middle Eocene age for the basal part. The lignite seams found within the Ogwashi-Asaba formation are commonly brownish to black in colour and vary in thickness from few millimetres to a maximum of 6m (Ogala, 2011). They are thinly laminated and fissile with leaf and woody fragments on fresh cleats. All the known seams of lignite within the Anambra basin of Nigeria occur west and east of the Niger, the thickest seams being located near Ogwashi-Asaba and Obomkpa area in Delta State. These areas have been explored by mapping and drilling.

The stratigraphic sequence of the area showing the layered seams of lignite underlained with the kaolin deposit along the river channel (Fig.5, 6 and 7).

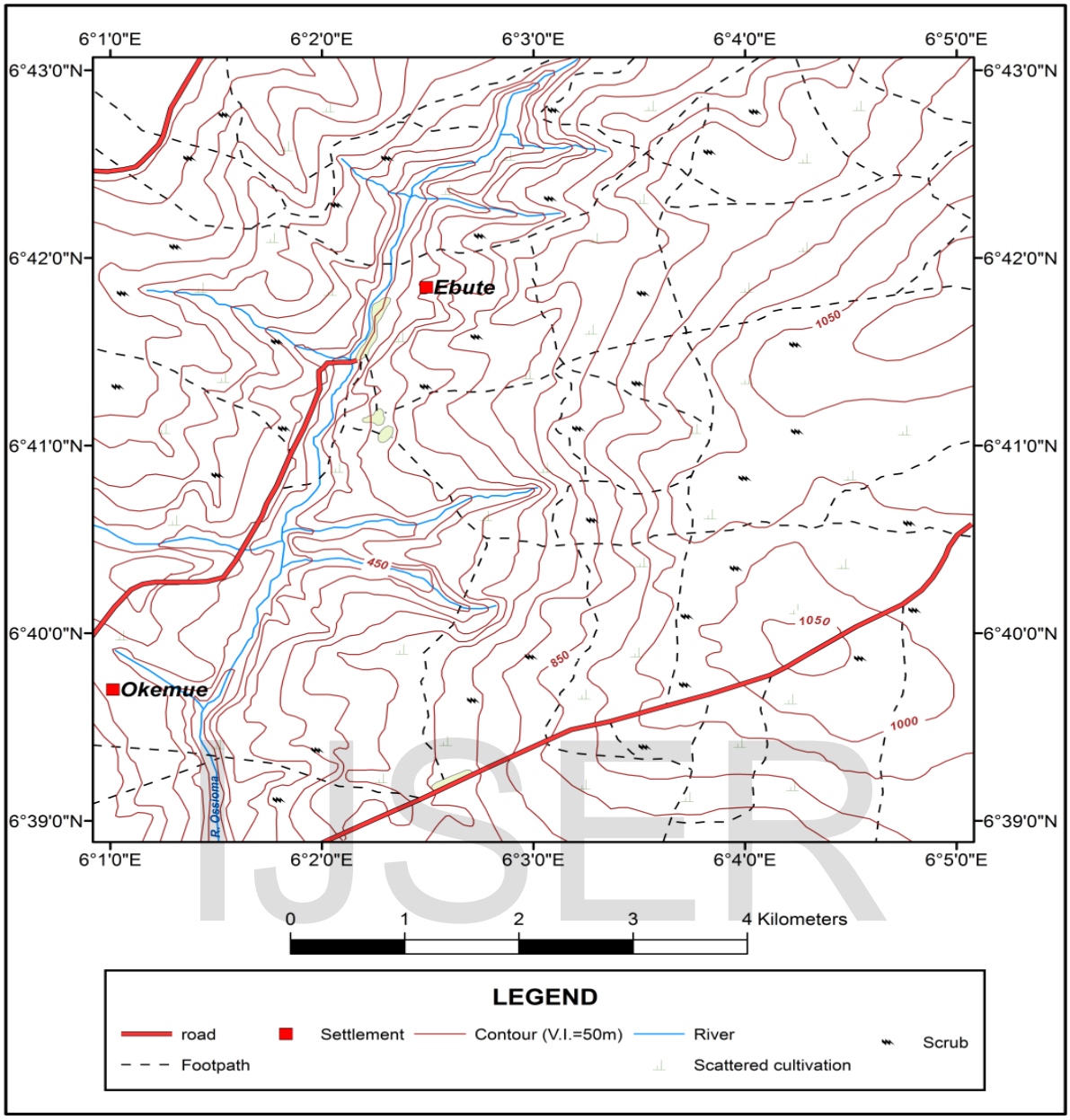


Fig. 1: Location map of the study area

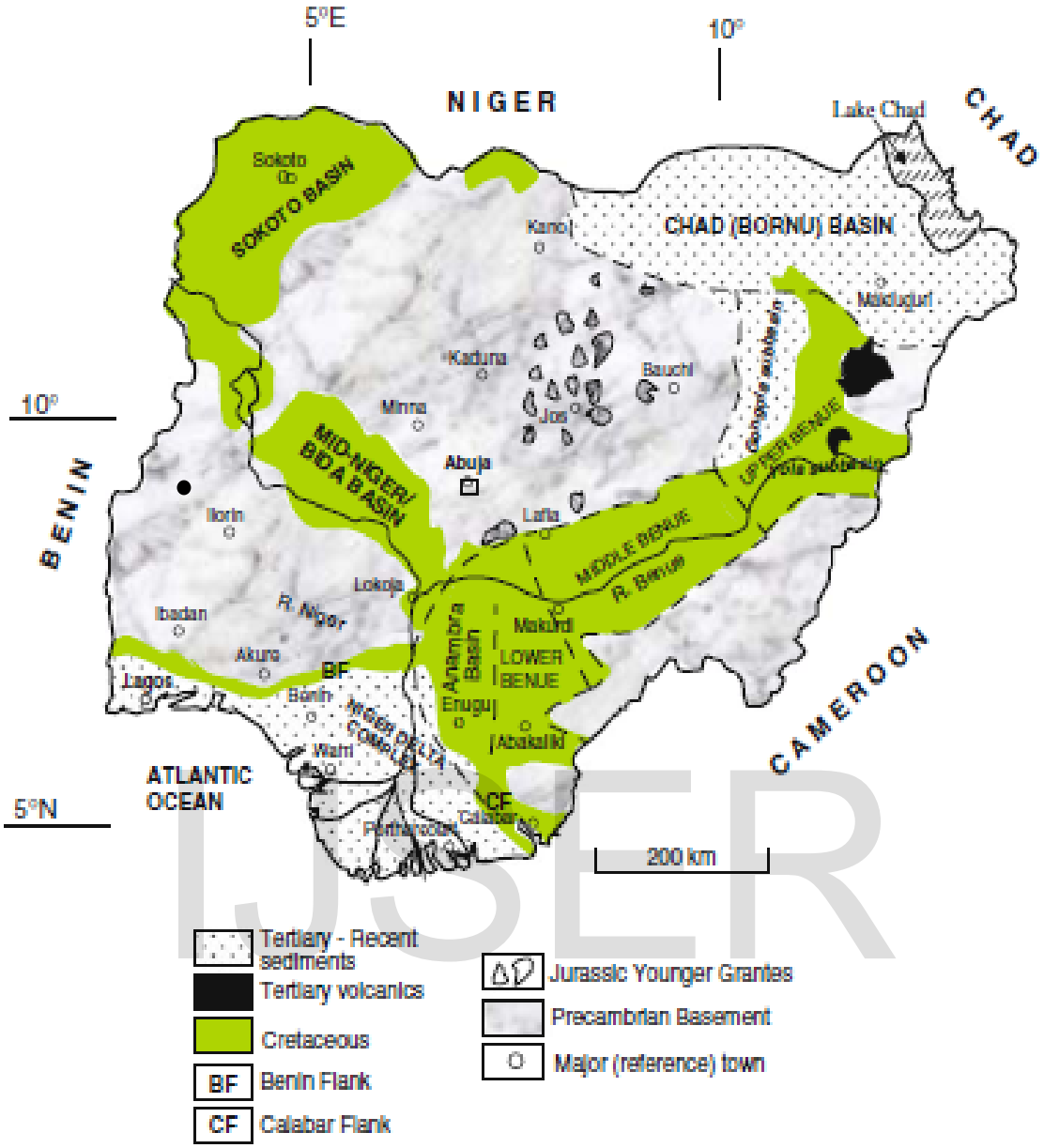


Fig. 2:Simplified map of the geology of Nigeria (Obaje, 2009).

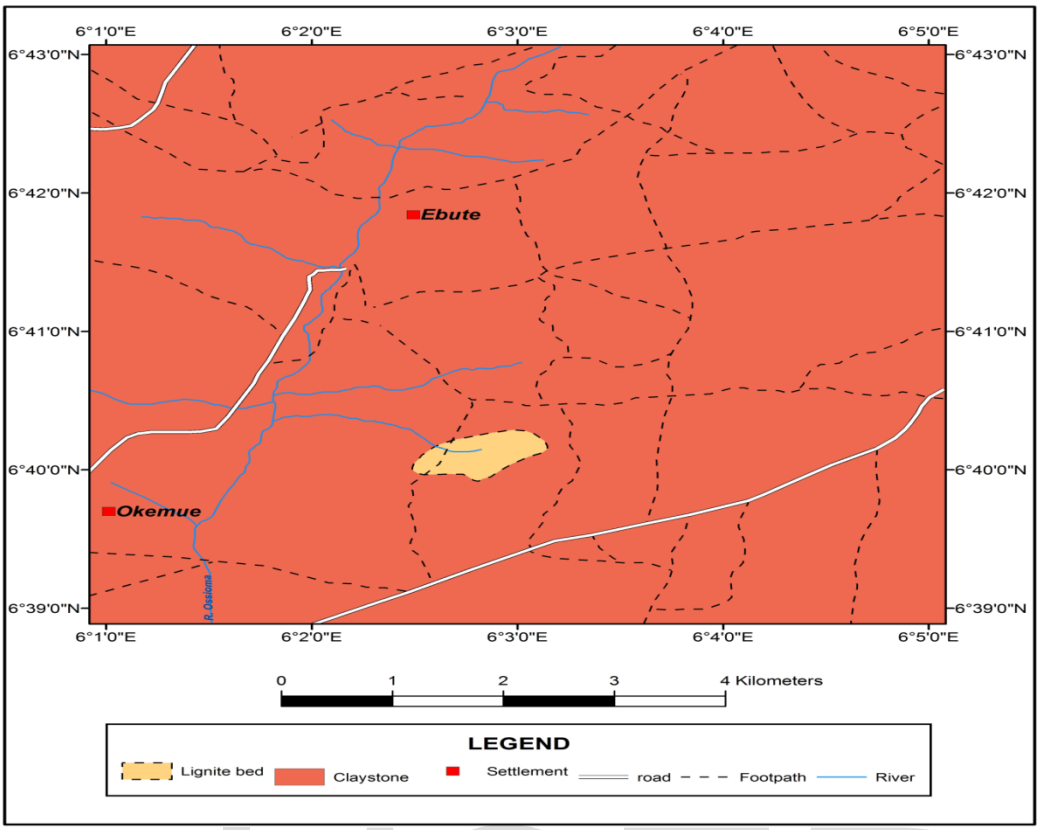


Fig.3: Geological map of the studied area around the kaolin deposit

| AGE | | FORMATION | LITHOLOGY | DEPOSITIONAL ENVIRONMENT | BASIN |
|---|---|---|---|---|---|
| Quaternary | | Benin Formation | Sandstones, Clay, Shales | Continental | Niger Delta Basin |
| Tertiary | Pliocene | | | | |
| | Miocene | | | | |
| | Oligocene | Ogwashi Asaba Formation | Clay, Shales, Sandstones, Lignite | Continental | |
| | Eocene | Ameki Formation/Nanka Sand | Sandstones, Cl ay, Shales, Limestone | Estuarine, Shallow marine | |
| | Paleocene | Imo Formation | Clay, Shales, Limestone, Sandstone, Marl | Shallow Marine, deltaic | |
| Upper Cretaceous | Maastrichtian | Nsukka Formation | Sandstones, Clays, Shales, Coals, Limestone | Fluvio - deltaic | Anambra Basin |
| | | Ajali Formation | Sandstones, Claystones | Fluvio – deltaic | |
| | | Mamu Formation | Sandstones, Clays, Coals | Shallow Marine, deltaic | |
| | Campanian | Enugu/Nkporo/Owelli Formation | Shales, Sandstones, Clay, ironstones, Siltstones. | Shallow Marine, deltaic | |
| | | MAJOR UNCONFORMITY | | | |
| | Santonian | Awgu Formation | Sandstones, Limestones, Clays, Coals, Siltstones | Shallow Marine, deltaic | Benue Trough |
| | Conician | | | | |
| Middle Cret. | Turonian | Eze -Aku Formation | Shales, Limestones, Sandstones | Shallow Marine | |
| | Cenomanian | Odukpani Formation | Sandstones, Limestones, Shales | Shallow Marine | |
| Lower Cret. | Albian | Asu River Group | Shales, Limestones, Sandstones | Shal low Marine | |
| Aptian | | MAJOR UNCONFORMITY | | | |
| | | Basement complex | Granites, Gneisses, Schists, Migmatites | Igneous, Metamorphic | |



Fig.4. Shows the stratigraphy of three basins in Southern Nigeria- Benue Trough, Anambra Basin and Niger Delta Basin (modified from Reyment, 1965).

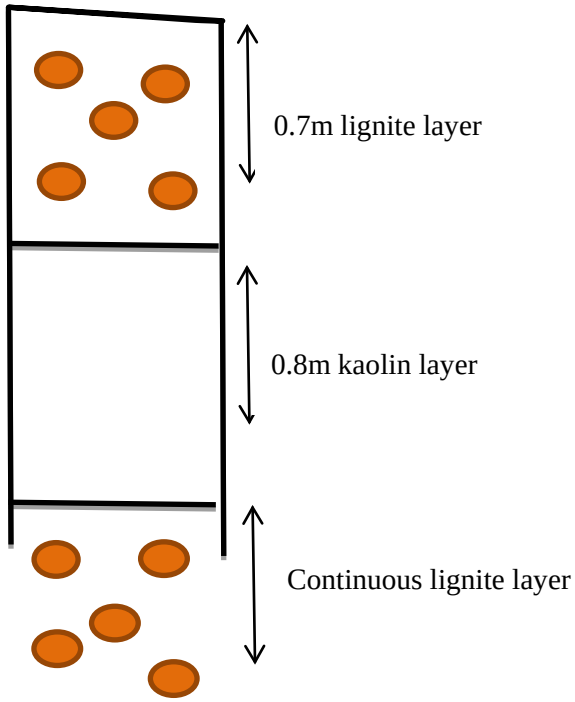


Fig.5. Typical Stratigraphic occurrence of the kaolin layer interbedded between two layered seams of lignite along the river channel



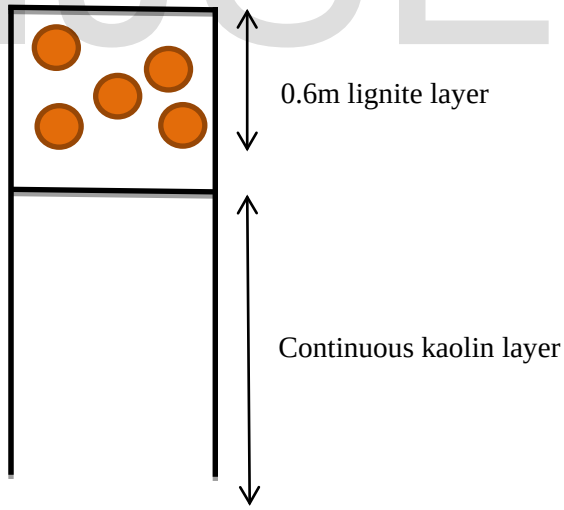


Fig.6. Typical Stratigraphic occurrence of a single layered seam of lignite above the continuous deposit of kaolin

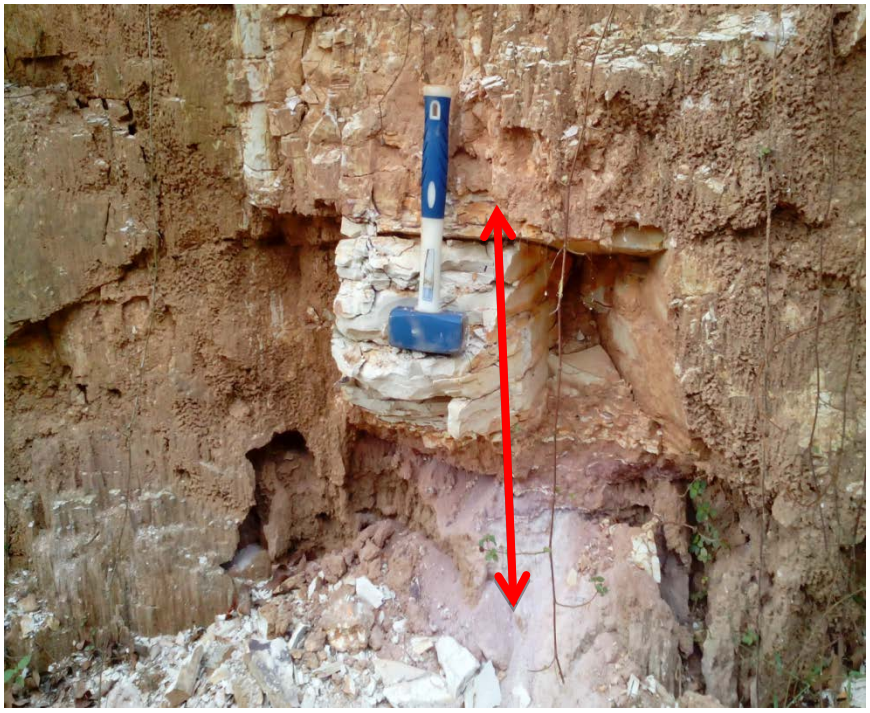

Fig.7: Field occurrence of the kaolin deposit in the study area with a considerable thickness of about 2.5m exposed at the surface

## 4. Results and Discussion

### 4.1. Mineralogy

The mineralogical assemblages of all the samples have been indicated against their diagnostic peaks. The main minerals identified by XRD in the kaolin deposits are kaolinite [$Al_2Si_2O_5(OH)_4$] and quartz[$SiO_2$]. Minerals of minor abundance as white mica, rutile, anatase and gibbsite might be heterogeneously distributed but not detected.These two minerals, kaolinite and quartz, comprise more than 98 wt.% of the three samples analysed. The samples analysed shows that kaolinite is the dominating mineral with lesser amount of quartz.

Under the optical microscope, kaolinite shows polycrystalline structure and forms the matrix. The analysed samples from Ugiamen kaolin deposit, the mica framework from the inherited lithologies is observed, and hence they do not show any reliquiar mica textures. The quartz grains do not show a well-developed outlines in all three samples analysed. There are some scattered specks of gibbsite crystals pseudomorph after kaolinite crystals which sometimes replace the earlier formed quartz grain, although this was not detected by XRD (Fig. 8, 9 and 10). Minerals such as crandallite-goyazite were not also observed by microscope most likely due to its highly fine crystal size. The kaolin deposits of Ugiamenmineralogically have abundance of polycrystalline quartz grains and also the presence of micas, this attribute makes it unique. Shallow burial of clay minerals usually account for the formation of illite mineral during diagenesis of clay minerals in sedimentary basin. The absence of illite confirmed deep burial of the clay occurrences in the study area. Also, the polycyclic lithology of coarsed-fine-coarsed sediments revealed high-low energy of paleo-current during the deposition of sediments of which the claystone generally represent the end of a depositional cycle.

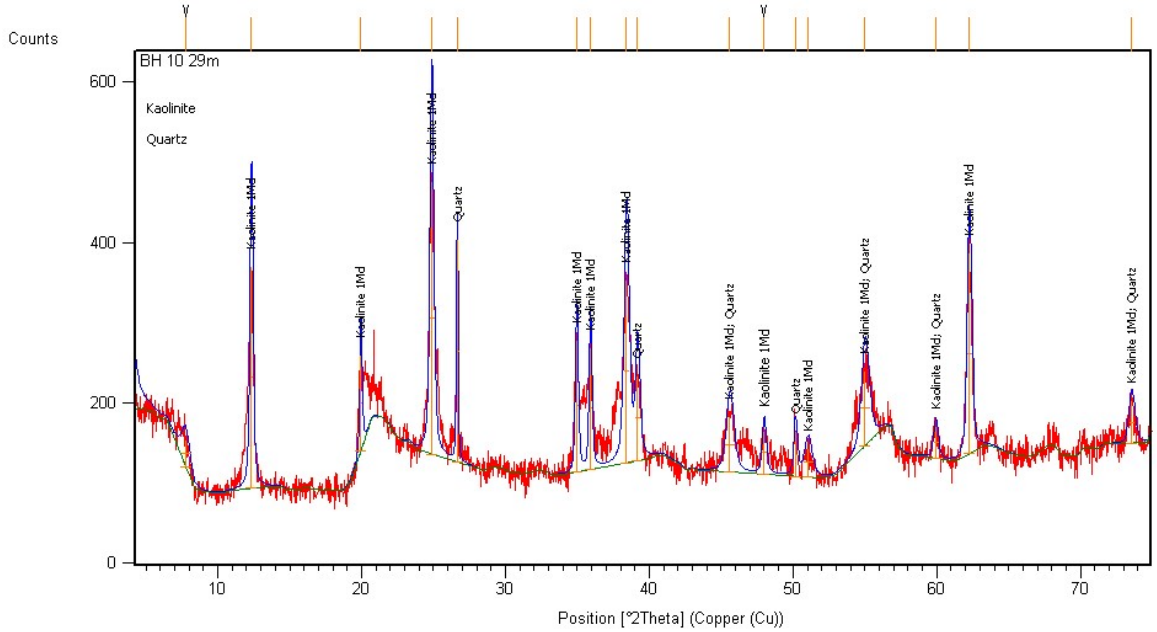


Fig. 8: X-ray diffraction patterns for bulk Ugiamen kaolin sample

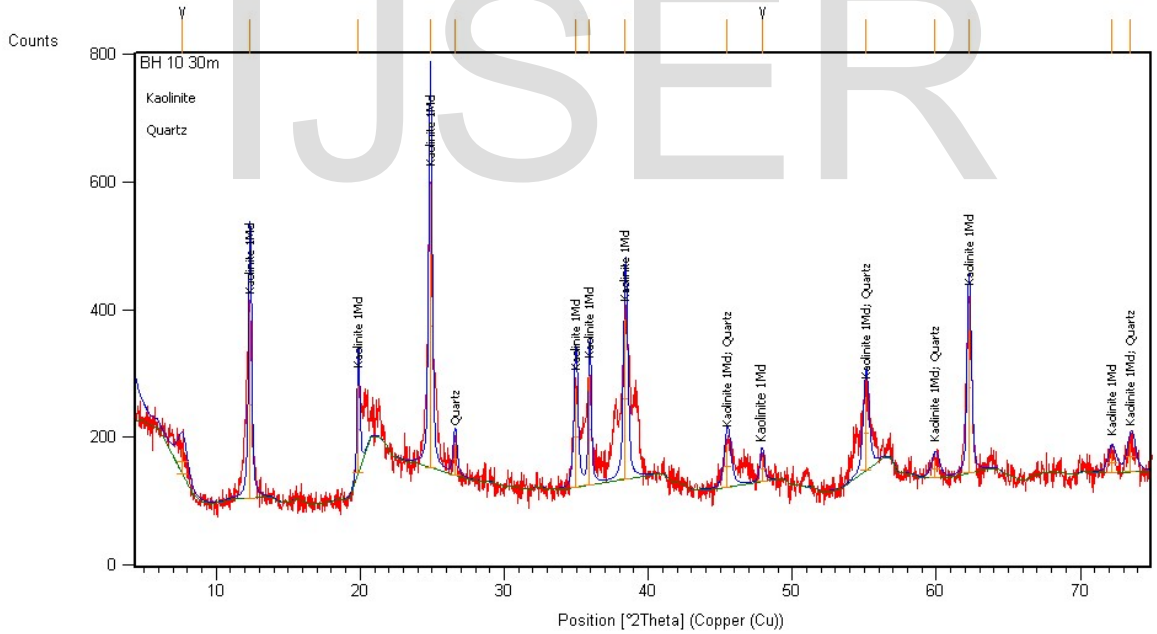


Fig. 9: X-ray diffraction patterns for bulk Ugiamen kaolin sample

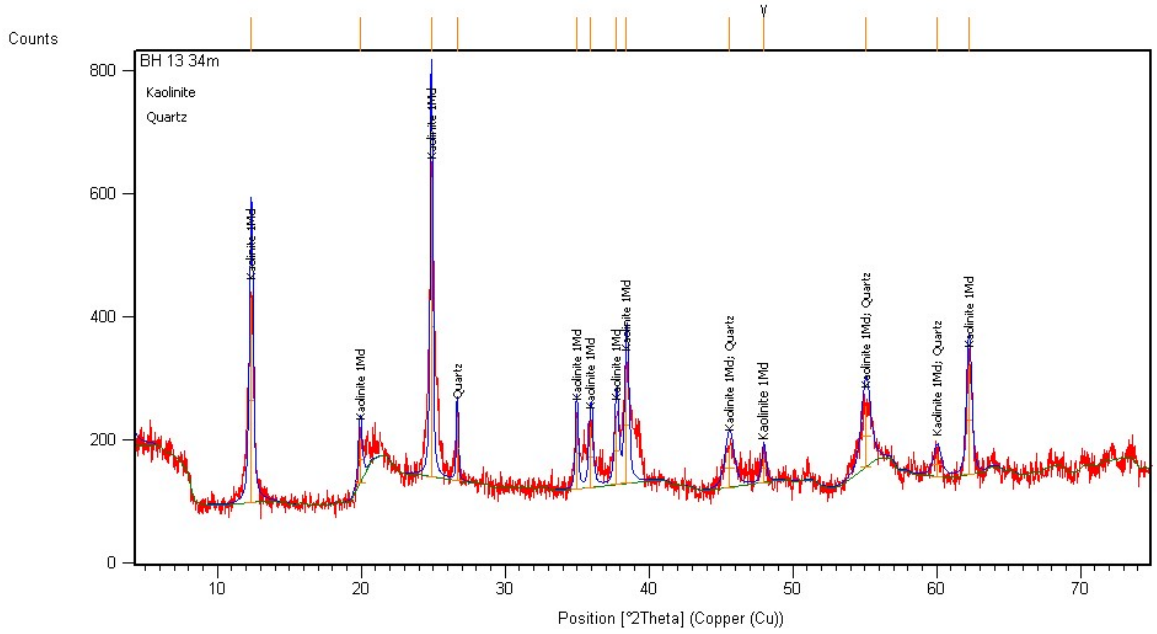


Fig. 10: X-ray diffraction patterns for bulk Ugiamen kaolin sample

## 4.2. Geochemistry

### *4.2.1. Major elements*

The geochemical analysis result of twelve kaolin samples collected from the study area show high value for $SiO_2$ ranging from between 41.04% and 74.48% and moderately high $Al_2O_3$ ranging between 14.95% and 33.58% and a low value for $Fe_2O_3$ ranging from 0.93% and 2.86%. Also the samples are significantly low in MgO, CaO, $Na_2O$ and $K_2O$ (Table 1). The low values for MgO, CaO, $Na_2O$ and $K_2O$ suggested the intense weathering and obliteration of feldspar during movement. These low values also indicate the source rock is not a carbonaceous or dolomitic in nature, and however indicates felsic origin.

The ternary diagrams below are showing the amounts of major oxides in the clay samples of the study area (Fig. 11). The triangular diagrams of A-CN-K and A-CNK-F were used to investigate the weathering process (Nesbit and Young 1996). The CIA amount has been evaluated using the equation: CIA= $[Al_2O_3/(Al_2O_3+CaO+Na_2O+K_2O)]*100$. By this equation, the value of CIA in the kaolin samples range from 99.1-99.8%. McLeman and Taylor (1991) regarded the CIA values of residual clays to be about 85-100%, which are related to the values of these samples. Also, based on the studies of the geochemistry of the weathering process, elements such as Na, Ca,, and Mg are leaching away during the process, as the degree of the weathering can be determined from the values of the remaining materials (Nyakairu et.al., 2001).

Also, the relationship in chemical composition can be seen on ternary diagrams of $SiO_2$- $Al_2O_3$- $Fe_2O_3$, $SiO_2$- $Al_2O_3$- $TiO_2$, $SiO_2$- $Al_2O_3$- $K_2O$, $SiO_2$- $Al_2O_3$- $Na_2O$, $SiO_2$- $Al_2O_3$- CaO, $SiO_2$- $Al_2O_3$- MgO and $SiO_2$- $Al_2O_3$- LOI (Fig. 11). From these ternary plots, all the kaolin sample plot in quite simple composition field. The kaolin deposits of Ugiamen have some little chemical differences compared to worldwide kaolin deposits of St. Austell-UK, kaolin of the Amazon, USA (Da Costa and Moraes, 1998, Sousa et. al., 2006).

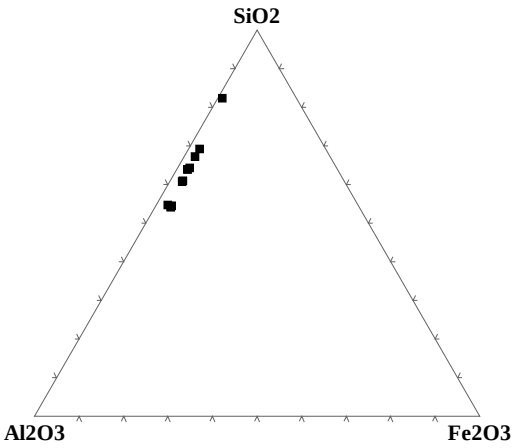


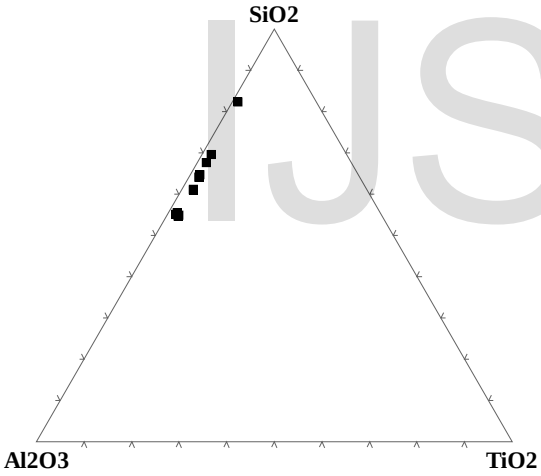

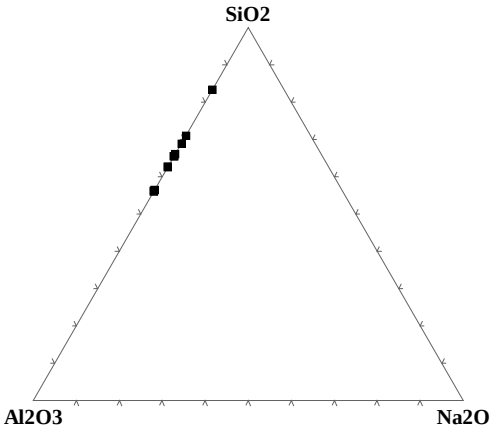
SiO2
Al2O3
Na2O

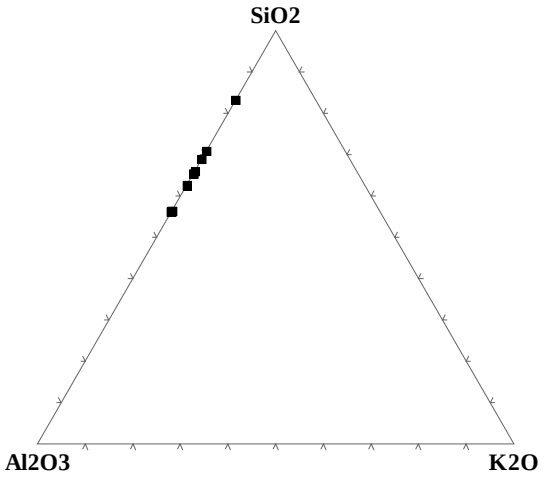
SiO2
Al2O3
K2O

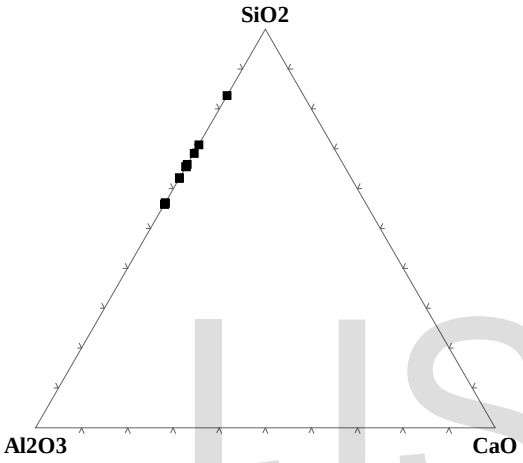
SiO2
Al2O3
CaO

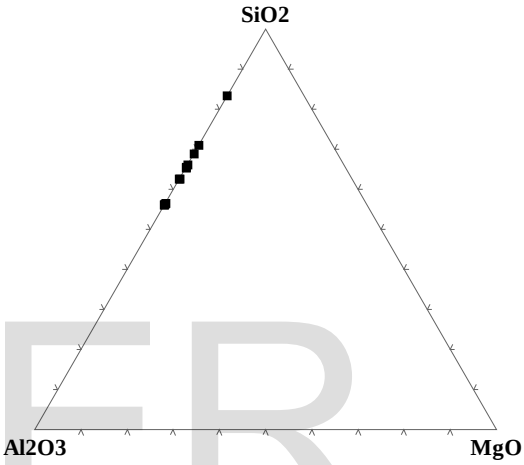
SiO2
Al2O3
MgO

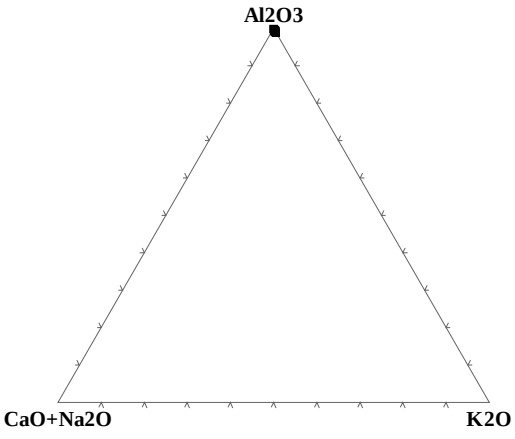
Al2O3
CaO+Na2O
K2O

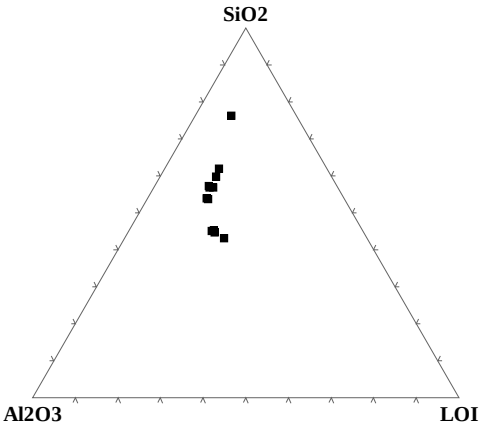
SiO2
Al2O3
LOI

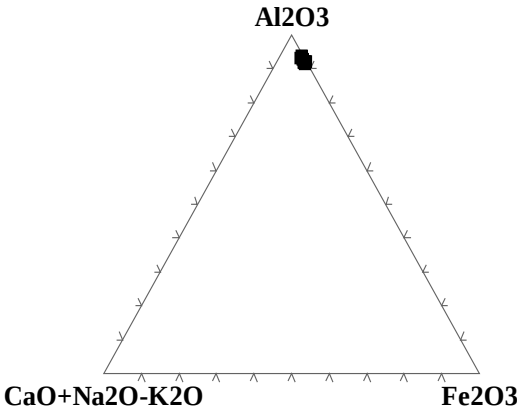


Fig.11:Triangular diagram between the main oxides. a The triangular diagram between the oxides of $SiO_2$-$Al_2O_3$-$Fe_2O_3$. bThe triangular diagram between the oxides of $SiO_2$- $Al_2O_3$- $TiO_2$. cThe triangular diagram between the oxides of $SiO_2$-$Al_2O_3$-$Na_2O$.d The triangular diagram between the oxides of $SiO_2$-$Al_2O_3$-$K_2O$. e The triangular diagram between the oxides of $SiO_2$-$Al_2O_3$-CaO. f The triangular diagram between the oxides of $SiO_2$-$Al_2O_3$-MgO. gThe triangular diagram between the oxides of $Al_2O_3$-CaO+$Na_2O$+$K_2O$- $Fe_2O_3$. hThe triangular diagram between the oxides of $Al_2O_3$-CaO+$Na_2O$-$K_2O$.iThe triangular diagram between the oxides of $SiO_2$-$Al_2O_3$-LOI.



***4.2.2. Trace elements***

For the trace elements composition of the kaolin samples, some trends are observed (Table 2). All the samples analyzed have a medium concentration of La (47.4-132.8ppm), Ba (113-179ppm), Sr (32.5-111.6ppm), Ce (89.8-256.1ppm) and Zr (273.9-833.7ppm) display varied interval of variation. Transition elements generally have low concentrations, except V (73-131ppm). Toxic elements such as As, Cd and Sb are absent or present with low concentration with low Pb concentration (5.3-20.1ppm).

Figure 12 shows the chemical differences based on the trace elements concentration of Ugiamen kaolin deposits, specifically the Ba-La-$P_2O_5$ and La-Ce-Nd ternary diagram. It must be noted that kaolin deposits which overlie either sedimentary rocks or gneisses are characterized by decreased concentration of trace elements when compared to the calculated Earth's crust abundances (Misra, 2012).

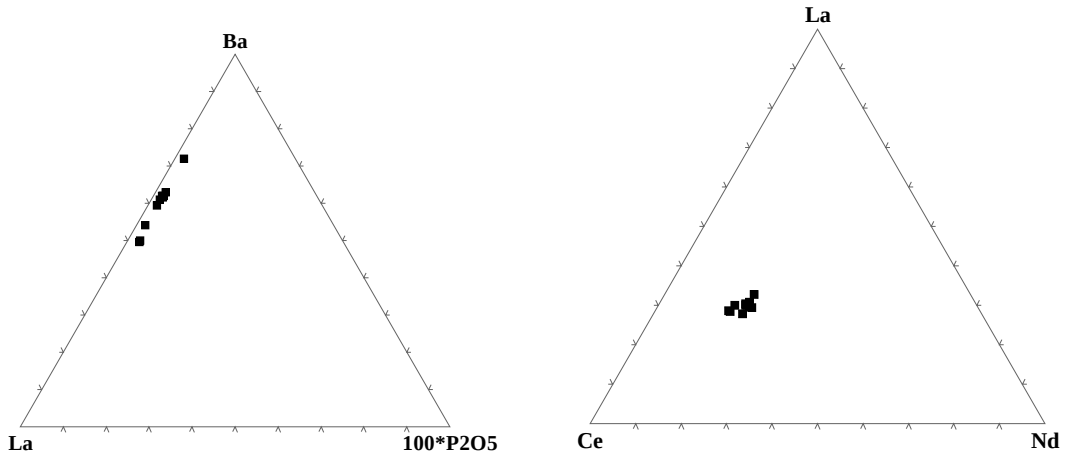


Fig. 12: The variation of the trace elements concentration of the kaolin samples

### *4.2.3. REE curve normalized to chondrites*

In the weathering process, the REE cations and minerals are released by hydrolysis from the original or parent material. Through the process of migration in water, the REE becomes concentrated in the favourable sites and afterward released from the unstable REE minerals. The REE in the crust are absorbed on clay particle fractions in the form of simple cations. The Ce-family (LREE, La, Ce, Pr, Nd) are more unsoluble to hydrolysis than the Y-family REE, more especially $Ce^{+4}$, which is the most unsoluble to hydrolysis than the other REE (Song Yunhun and Shen Lipu, 1987).



The normalized curve for REEs in fig. 13 confirmed by the fact that the kaolin samples are relatively enriched in the Ce-family REE, Ce content is the highest at the top of the kaolin samples and the Ce-family REE tend to become enriched during weathering processes. The curve also give a slightly negative europium anomaly and most of them display a strongly positive Ce-anomaly. The HREEs display an apparent enrichment from Lu to Gd. This trends indicates evident characteristic feature of the lateritic weathering and also the influence of acidic parent rock. This also confirm the origin of the kaolin deposits. The negative anomaly of Eu can be associated with an atmospheric or hydrothermal origin (Rollinsn 1993). The enrichment of La can be also be associated to the alteration of sericite in the region (Tsuzuki and Mizutani, 1969).

In general, the chondrite-normalized REE pattern with Eu negative and Ce positive anomalies and slightly positive anomalies of La and Gd demonstrates the weathering effect of acidic source rocks for the kaolin deposit in the study area.

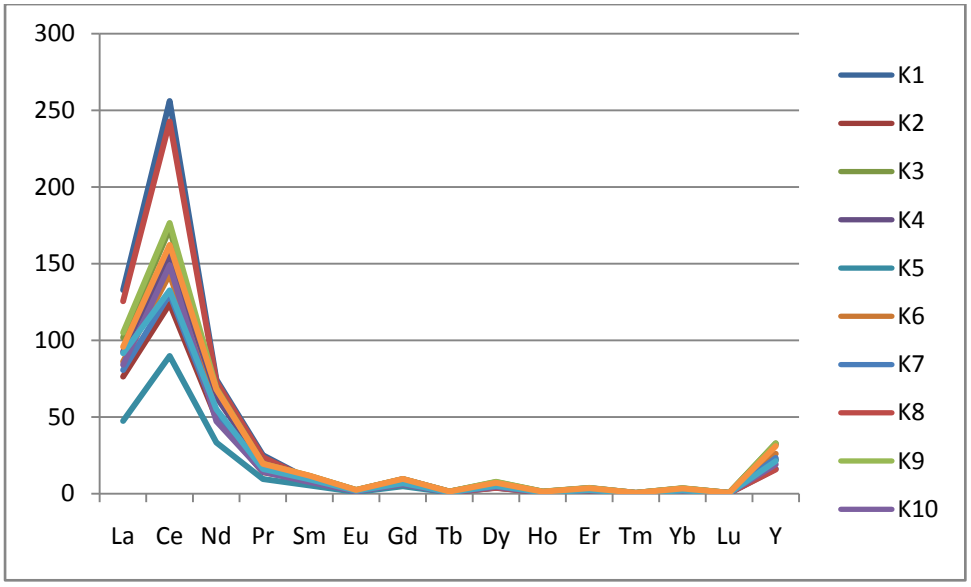


Fig.13: REE pattern of Ugiamen kaolin samples normalized, the kaolins show a general LREE enrichment with a Ce positive anomaly. Chondrite-normalizing values are from McDonough and Sun 1995

## 5. Conclusions



Geological mapping has identified the occurrence of kaolinite interbedded with the occurrence of lignite in the study area. The kaolin deposits are predominantly developed on the clay-bearing parent materials of the Tertiary age from the OgwashiAsaba Formation. This kaolinite is believed to be formed by enhanced weathering of claystones consisting potassium-enriched minerals, such as muscovite and feldspar. Mineralogical and geochemical analysis carried out on the kaolin samples shows that kaolinite (up to 85%) is the dorminating mineral, followed by quartz; these are the main mineralogical phases in these deposit. Accessory minerals such as muscovite, rutile, anatase and gibbsite were heterogeneously identified in hand specimen as impurities. The kaolin are $SiO_2$, $Al_2O_3$ and LOI enriched; with low values of MgO, CaO and $Na_2O$ indicative of intense weathering and obliteration of feldspar. The higher $SiO_2$content is a desirable potential for the manufacture of floor tile and other ceramic products. Also the high $Al_2O_3$ content is related to the amount of muscovite present in the samples. The ternary diagrams of A-CN-K and A-CNK-F, the CIA index explain a relatively intense weathering process.

In the REE chondrite-normalized plot, the kaolin samples indicate enrichment of LREE in comparison to the HREE, which show a slightly negative Eu anomaly. This trend indicates evident characteristic feature of the lateritic weathering and also the influence of the acidic nature of the source rock. Based on the geochemical and mineralogical characteristics of these deposits, we infer that these studied material which is sand-poor, silica-

rich are very good materials for industrial applications such for the manufacture of stoneware tiles and other fine ceramics, paint and paper coating. These raw materials are easy to access and economical to process due to the mineralogy and abundance of these materials for local production.

**Acknowledgments** We are grateful to Jidet Nigeria Limited for their support. We would like to thank our colleagues I. O. Babatunde and O. O. Odebunmi for their constructive comment and research assistance.

This research did not receive any specific grant from funding agencies in the public, commercial, or not-for-profit sectors.

**References**

Akhirevbulu, O., & Ogunbajo, M. (2011). The Geotechnical Properties Of Clay Occurrences Around Kutigi Central Bida Basin, Nigeria. *Ethiopian Journal of Environmental Studies and Management*, *4*(1).

Benkhelil, J. (1989). The origin and evolution of the Cretaceous Benue Trough (Nigeria). *Journal of African Earth Sciences (and the Middle East)*, *8*(2), 251-282.

Bundy, W. M. (1990). Diverse Industrial Applications of Kaolin. *Clay Miner. Soc. Spec. Pub.*(1), 43-73.

Da Costa, M., & Moraes, E. (1998). Mineralogy, geochemistry and genesis of kaolins from the Amazon region. *Mineralium Deposita*, *33*(3), 283-297.

Jan du Chêne, R., Onyike, M., & Sowunmi, M. (1978). Some new Eocene pollen of the Ogwashi-Asaba Formation, southeastern Nigeria. *Revista Espanola de Micropaleontologia*, *10*(2), 285-322.

Kogbe, C. A. (1976). *Geology of Nigeria*: Elizabethan Publishing Company.

McDonough, W. F., & Sun, S.-S. (1995). The composition of the Earth. *Chemical geology*, *120*(3-4), 223-253.

McLennan, S., & Taylor, S. (1991). Sedimentary rocks and crustal evolution: tectonic setting and secular trends. *The Journal of Geology*, *99*(1), 1-21.

Misra, K. (2012). *Understanding mineral deposits*: Springer Science & Business Media.

Murray, H., & Keller, W. (1993). Kaolins, kaolins, and kaolins. Pp. 1À25 in: Kaolin Genesis and Utilization (H. Murray, W. Bundy & C. Harvey, editors). Special Publication, 1. *The Clay Minerals Society, Boulder, Colorado, USA*.

Nesbitt, H. W., & Young, G. M. (1996). Petrogenesis of sediments in the absence of chemical weathering: effects of abrasion and sorting on bulk composition and mineralogy. *Sedimentology*, *43*(2), 341-358.

Nwachukwu, S. (1972). The tectonic evolution of the the southern portion of the Benue Trough, Nigeria. *Geological magazine*, *109*(05), 411-419.

Nyakairu, G. W., Koeberl, C., & Kurzweil, H. (2001). The Buwambo kaolin deposit in central Uganda: Mineralogical and chemical composition. *Geochemical Journal*, *35*(4), 245-256.

Ogala, J. (2011). Source rock potential and thermal maturity of the Tertiary lignite series in the Ogwashi-Asaba Formation, Southern Nigeria. *Asian Journal of Earth Sciences*, *4*(3), 157.

Olade, M. (1975). Evolution of Nigeria's Benue Trough (Aulacogen): a tectonic model. *Geological magazine*, *112*(06), 575-583.

Rashad, A. M. (2013). Metakaolin as cementitious material: History, scours, production and composition–A comprehensive overview. *Construction and building materials*, *41*, 303-318.

Reyment, R. A. (1965). *Aspects of the geology of Nigeria: The stratigraphy of the Cretaceous and Cenozoic deposits*: Ibadan university press.

Rollinson, H. (1993). Using stable isotope data. *Using Geochemical Data: Evaluation, Presentation, Interpretation: Geochemistry Series, Longman Scientific and Technical co-published with Wiley and Sons, New York*, 266-315.

Short, K., & Stauble, A. (1967). Outline of geology of Niger Delta. *AAPG bulletin*, *51*(5), 761-779.

Sousa, D. J. L. d., Varajão, A. F. D. C., & Yvon, J. (2006). Geochemical evolution of the Capim River kaolin, northern Brazil. *Journal of Geochemical Exploration*, *88*(1), 329-331.

Tsuzuki, Y., & Mizutani, S. (1969). *Kinetics of hydrothermal alteration of sericite and its application to the study of alteration zoning*. Paper presented at the Proceedings International Clay Conference.

Yunhua, S., & Lipu, S. (1987). REE geochemistry of the weathered crust of acid volcanic rocks—An experimental study. *Chinese Journal of Geochemistry*, *6*(2), 165-176.

## APPENDIX

**Table 1: Major elements content (wt. %) of Ugiamen clay**

| Oxides | K1 | K2 | K3 | K4 | K5 | K6 | K7 | K8 | K9 | K10 | K11 | E2 |
|---|---|---|---|---|---|---|---|---|---|---|---|---|
| $SiO_2$ | 42.83 | 59.28 | 50.98 | 54.83 | 74.48 | 54.31 | 57.31 | 41.04 | 51.52 | 43 | 42.99 | 54.57 |
| $Al_2O_3$ | 33.53 | 24.24 | 30.34 | 28.88 | 14.95 | 27.92 | 25.87 | 31.9 | 30.09 | 33.1 | 33.58 | 28.87 |
| $Fe_2O_3$ | 2.77 | 2.02 | 2.41 | 2 | 0.93 | 2.29 | 2.11 | 2.63 | 2.44 | 2.86 | 2.01 | 2 |
| MgO | 0.06 | 0.07 | 0.07 | 0.07 | 0.05 | 0.08 | 0.07 | 0.05 | 0.07 | 0.08 | 0.07 | 0.07 |
| CaO | 0.02 | 0.03 | 0.03 | 0.01 | 0.02 | 0.02 | 0.02 | 0.02 | 0.01 | 0.02 | 0.02 | 0.01 |
| $Na_2O$ | <0.01 | <0.01 | 0.01 | <0.01 | <0.01 | <0.01 | <0.01 | <0.01 | <0.01 | <0.01 | <0.01 | <0.01 |
| $K_2O$ | 0.06 | 0.16 | 0.21 | 0.16 | 0.16 | 0.18 | 0.17 | 0.04 | 0.21 | 0.19 | 0.13 | 0.17 |
| $TiO_2$ | 1.96 | 1.65 | 2.06 | 1.76 | 1.05 | 1.74 | 1.65 | 1.87 | 2.07 | 1.5 | 1.37 | 1.78 |
| $P_2O_5$ | 0.08 | 0.05 | 0.06 | 0.05 | 0.04 | 0.06 | 0.05 | 0.08 | 0.07 | 0.05 | 0.04 | 0.05 |
| MnO | <0.01 | <0.01 | <0.01 | <0.01 | <0.01 | <0.01 | <0.01 | <0.01 | <0.01 | <0.01 | <0.01 | <0.01 |
| $Cr_2O_3$ | 0.02 | 0.012 | 0.024 | 0.015 | 0.008 | 0.014 | 0.013 | 0.019 | 0.025 | 0.013 | 0.013 | 0.015 |
| LOI | 18.5 | 12.3 | 13.6 | 12.1 | 8.2 | 13.2 | 12.6 | 22.2 | 13.3 | 19 | 19.6 | 12.3 |
| Total | 99.83 | 99.812 | 99.794 | 99.875 | 99.888 | 99.814 | 99.863 | 99.849 | 99.805 | 99.813 | 99.823 | 99.835 |

**Table 2: Trace elements content (wt. ppm) of Ugiamen clay**

| Elements | K1 | K2 | K3 | K4 | K5 | K6 | K7 | K8 | K9 | K10 | K11 | E2 |
|---|---|---|---|---|---|---|---|---|---|---|---|---|
| Ni | 26 | <20 | 22 | <20 | 21 | <20 | <20 | 23 | <20 | 27 | 28 | <20 |
| Sc | 14 | 14 | 19 | 15 | 8 | 15 | 14 | 13 | 19 | 16 | 16 | 15 |
| Ba | 141 | 132 | 175 | 153 | 132 | 157 | 139 | 131 | 179 | 145 | 113 | 148 |
| Be | 2 | 1 | 2 | 1 | <1 | <1 | 3 | 1 | 1 | 1 | 2 | 3 |
| Co | 3.3 | 2.6 | 2.5 | 2.7 | 6.7 | 2.7 | 2.2 | 2.4 | 2.7 | 2.9 | 2.7 | 2.3 |
| Cs | 0.2 | 1.5 | 0.8 | 0.9 | 0.7 | 1.9 | 1.8 | 0.2 | 0.9 | 1.8 | 1.4 | 0.9 |
| Ga | 44.2 | 34.3 | 41.9 | 32.9 | 16.5 | 38.6 | 36.8 | 42.6 | 41 | 46.8 | 43.2 | 34.8 |
| Hf | 7.5 | 20.6 | 12.8 | 10.7 | 14.7 | 16.7 | 17.7 | 7.5 | 13.9 | 7.4 | 7.3 | 10.2 |
| Nb | 67.7 | 66.1 | 78.1 | 61.5 | 30.7 | 68.1 | 61.9 | 56.8 | 78.1 | 71.3 | 68.6 | 59.1 |
| Rb | 3.5 | 11.9 | 11.1 | 8.5 | 8.3 | 13.2 | 12.8 | 3.2 | 11.5 | 12.5 | 10.5 | 9.2 |
| Sn | 5 | 5 | 7 | 5 | 2 | 6 | 6 | 5 | 8 | 6 | 6 | 5 |
| Sr | 111.6 | 55.9 | 82.6 | 60.6 | 32.5 | 69.4 | 62.1 | 107.2 | 88.2 | 71.4 | 65.1 | 65.3 |
| Ta | 3.6 | 4.1 | 4.9 | 3.7 | 2 | 4.2 | 3.8 | 3.5 | 4.8 | 4 | 4.3 | 3.5 |
| Th | 20.6 | 21.4 | 29.6 | 21.7 | 12.2 | 22.4 | 22.3 | 20.9 | 31.7 | 28.1 | 17.1 | 22.6 |
| U | 2.6 | 5.1 | 4.6 | 4.5 | 2.5 | 5.4 | 4.7 | 2.3 | 4.8 | 3.1 | 2.8 | 4.2 |
| V | 118 | 98 | 128 | 89 | 73 | 110 | 102 | 113 | 131 | 122 | 99 | 97 |

| | | | | | | | | | | | | |
|---|---|---|---|---|---|---|---|---|---|---|---|---|
| W | 2.5 | 2.5 | 1.9 | 2.2 | 1.1 | 2 | 2.4 | 1.9 | 2.3 | 2.3 | 1.6 | 2.5 |
| Zr | 300 | 833.7 | 517.1 | 417.8 | 606.7 | 674.9 | 711.9 | 294.8 | 543.2 | 273.9 | 275.9 | 400.8 |
| Y | 16.2 | 21.9 | 32.9 | 31.9 | 22.2 | 26 | 23.3 | 15.7 | 32.7 | 19.1 | 21.2 | 31 |
| La | 132.8 | 76.3 | 101.8 | 92.5 | 47.4 | 86.1 | 80.6 | 125.5 | 105 | 84 | 91.6 | 95.7 |
| Ce | 256.1 | 123.8 | 172.7 | 156.2 | 89.8 | 143 | 130.2 | 242.7 | 176.6 | 149 | 132.6 | 162.2 |
| Pr | 25.01 | 14.05 | 19.13 | 18.5 | 9.52 | 15.9 | 14.73 | 23.68 | 19.61 | 14.17 | 16.07 | 19.35 |
| Nd | 74.4 | 49.1 | 65.5 | 63 | 33.3 | 53.4 | 51.4 | 72.9 | 68.7 | 47.2 | 55 | 67.9 |
| Sm | 9.2 | 8.44 | 11.55 | 11.35 | 5.32 | 9.03 | 8.79 | 9.24 | 11.62 | 7.48 | 9.25 | 11.66 |
| Eu | 1.89 | 1.58 | 2.32 | 2.3 | 1.06 | 1.86 | 1.68 | 1.7 | 2.46 | 1.43 | 1.84 | 2.34 |
| Gd | 6.87 | 6.78 | 9.4 | 9.49 | 4.78 | 7.54 | 7.44 | 7.03 | 9.58 | 6.02 | 6.82 | 9.62 |
| Tb | 0.81 | 0.94 | 1.35 | 1.34 | 0.71 | 1.08 | 1.01 | 0.79 | 1.39 | 0.82 | 0.95 | 1.38 |
| Dy | 3.96 | 5.03 | 7.54 | 7.05 | 3.92 | 5.71 | 5.47 | 3.77 | 7.73 | 4.36 | 5.06 | 7.12 |
| Ho | 0.68 | 0.89 | 1.36 | 1.28 | 0.73 | 1.07 | 0.98 | 0.65 | 1.36 | 0.75 | 0.88 | 1.25 |
| Er | 1.79 | 2.44 | 3.58 | 3.63 | 2.03 | 2.82 | 2.65 | 1.9 | 3.77 | 2.11 | 2.29 | 3.52 |
| Tm | 0.28 | 0.38 | 0.55 | 0.54 | 0.32 | 0.4 | 0.4 | 0.28 | 0.57 | 0.29 | 0.33 | 0.52 |
| Yb | 1.89 | 2.49 | 3.45 | 3.29 | 2.08 | 2.89 | 2.54 | 1.76 | 3.6 | 1.83 | 2.07 | 3.28 |
| Lu | 0.29 | 0.38 | 0.54 | 0.51 | 0.32 | 0.4 | 0.4 | 0.29 | 0.56 | 0.28 | 0.31 | 0.5 |
| Mo | 0.2 | 0.3 | 0.1 | 0.1 | 0.1 | 0.2 | 0.3 | 0.1 | 0.1 | 0.5 | 0.2 | <0.1 |
| Cu | 9.7 | 14.5 | 23.2 | 7.9 | 14.6 | 17.4 | 16.7 | 6.5 | 21.9 | 14.9 | 13.1 | 6.9 |

| | | | | | | | | | | | | |
|---|---|---|---|---|---|---|---|---|---|---|---|---|
| Pb | 6.8 | 10.5 | 16.6 | 6.3 | 8.1 | 10.5 | 9.6 | 5.3 | 20.1 | 9.1 | 11.7 | 6.8 |
| Zn | 7 | 7 | 7 | 16 | 70 | 8 | 7 | 4 | 5 | 7 | 8 | 15 |
| Ni | 0.6 | 0.7 | 0.7 | 1.1 | 6.3 | 0.7 | 0.8 | 0.8 | 0.6 | 1 | 0.8 | 0.9 |
| As | <0.5 | <0.5 | <0.5 | <0.5 | <0.5 | <0.5 | <0.5 | <0.5 | <0.5 | <0.5 | <0.5 | <0.5 |
| Cd | <0.1 | <0.1 | <0.1 | <0.1 | <0.1 | <0.1 | <0.1 | <0.1 | <0.1 | <0.1 | <0.1 | <0.1 |
| Sb | <0.1 | <0.1 | <0.1 | <0.1 | <0.1 | <0.1 | <0.1 | <0.1 | <0.1 | <0.1 | <0.1 | <0.1 |
| Bi | <0.1 | <0.1 | <0.1 | <0.1 | <0.1 | <0.1 | <0.1 | <0.1 | <0.1 | <0.1 | <0.1 | <0.1 |
| Ag | <0.1 | <0.1 | <0.1 | <0.1 | <0.1 | <0.1 | <0.1 | <0.1 | <0.1 | <0.1 | <0.1 | <0.1 |
| Au | <0.5 | 1.1 | <0.5 | <0.5 | <0.5 | <0.5 | 0.9 | <0.5 | 0.7 | 1.1 | <0.5 | <0.5 |
| Hg | 0.01 | 0.1 | 0.04 | 0.06 | 0.03 | 0.11 | 0.09 | 0.01 | 0.03 | 0.19 | 0.11 | 0.04 |
| Ti | <0.1 | <0.1 | <0.1 | <0.1 | <0.1 | <0.1 | <0.1 | <0.1 | <0.1 | <0.1 | <0.1 | <0.1 |
| Se | <0.5 | <0.5 | <0.5 | <0.5 | <0.5 | <0.5 | <0.5 | <0.5 | <0.5 | <0.5 | <0.5 | <0.5 |